Available online at www.sciencedirect.com
SCIENCE DIRECT
Journal of Sound and Vibration 263 (2003) 415–442
JOURNAL OF SOUND AND VIBRATION
www.elsevier.com/locate/jsvi

An efficient differential quadrature methodology for free vibration analysis of arbitrary straight-sided quadrilateral thin plates

G. Karami*, P. Malekzadeh

Department of Mechanical Engineering, School of Engineering, Shiraz University, Shiraz 71345, Iran

Received 22 October 2001; accepted 26 June 2002

Abstract

In this paper, a new differential quadrature (DQ) methodology is employed to study free vibration of irregular quadrilateral straight-sided thin plates. A four-nodded super element is used to map the irregular physical domain into a square domain in the computational domain. Second order transformation schemes with relative ease and less computation are employed to transform the fourth order governing equation of thin plates between the two domains. The only degree of freedom within the domain is the displacement, whereas along the boundaries, the displacement as well as the second order derivative of the displacement with respect to associated normal co-ordinate variable in computational domain are the two degrees of freedom. Implementing the method, the formulation for the DQ method for the free vibration analysis of plates of straight-sided shapes was presented together with the implementation procedure for the different boundary conditions. To demonstrate the accuracy, convergency and stability of the new methodology, detail studies are made on isotropic plates at acute angles with different geometries, boundary and loading conditions including DQ free-edge boundary condition implementations. Accurate results even with fewer degrees of freedom than for those of comparable numerical algorithms were achieved.

1. Introduction

It is now more than a decade since the differential quadrature method (DQM) has established itself as a numerical algorithm in engineering analysis. A survey on the early stages of the method development and its applications was presented by Bert and Malik [1]. One troublesome point in

*Corresponding author. Current address: Department of Mechanical Engineering, University of Wyoming, P.O. Box 3295, Laramie, WY 82071, USA. Tel.: +1-307-766-2186; fax: +1-307-766-2695.
E-mail address: karami@who.edu (G. Karami).

PII: S0022-460X(02)01062-3

the classical application of DQM is the difficulty of impositioning of the boundary conditions for problems having governing differential equations with at least two boundary conditions at the boundary point. To overcome this difficulty, different methodologies were introduced. An approximate scheme to be referred to as "δ method" introduced by Bert et al. [2] was subsequently found [3]. It is not equally successful for all structural components with different boundary conditions if δ is not assumed to be very small. On the other hand, if δ is taken too small, the solutions may be subjected to oscillations. Also, in practice, the introduction of two end grid points separated by a small distance δ causes erroneous behavior. Furthermore, the method is not quite convenient and accurate to be implemented in the differential quadrature element method (DQEM). In searching for alternative schemes, Malik and Bert [4] have extended the work of Wang and Bert [5] to implement the boundary conditions by building them into the weighting coefficients. This method can be applied only for those types of boundary conditions that do not have mixed derivatives. In a third methodology, the slope on the boundary is chosen as a degree of freedom (see, for examples, Refs. [6–10]). In all the works where that slope is chosen as a degree of freedom, the weighting coefficients have been obtained by reformulating the DQ rule. Except for the works of Wu and Liu [8–10], a direct linear solver was used to obtain the weighting coefficients. Determination of weighting coefficients in such a manner obstructs DQM accuracy.

In the present methodology, the weighting coefficients are not exclusive and any of those schemes used in conventional DQM for determination of the weighting coefficients may be employed. The generalized DQM (GDQM) claimed to be the most computationally efficient and accurate method [1], can be easily used. The applicabilities of the methodology to beams and rectangular plates were demonstrated through previous studies [11,12]. It has been proved that for cases where conventional DQMs have not yielded a convergence trend or have erratic behavior, the new methodology yields accurate results with an excellent convergency behavior.

Most of the works on DQM structural analysis have been carried out for structures having boundaries such as rectangular, circular or cylindrical shapes where natural curvilinear coordinate systems can easily be defined. Few have considered the irregular structural problems. Wang et al. [13] have used DQM for buckling and free vibration analysis of thin skew plates for the first time. They have considered S–S–S–S and C–C–C–C boundary conditions. Oblique reference axes were used to transform the governing equations and the related boundary conditions together with the δ method for boundary condition implementations. Bert and Malik [14] have studied the free vibration of irregular thin clamped and simply supported plates. A δ method is used to implement the boundary conditions and therefore it is not convenient to be used for large scale structures that need domain decomposition. Four-nodded and also eight-nodded quadrature formulas have been used, respectively, by Liew and Han [15] and Han and Liew [16] to solve straight-sided and curved-sided Reissner/Mindlin plates. They have further employed their algorithms for bending analysis of thick skew plates [17,18].

In association with the DQ method, the differential cubature (DC) method has also been introduced. Following the introduction of this method by Civan [19], Liew and Liu [20] have employed the method for static analysis of arbitrary thin plates with simply supported and clamped boundary conditions. In another application of the method, Liu and Liew [21] have considered the static analysis of thick plates.

In this paper, other than the applicabilities of the new DQ methodology, its efficiency as an alternative numerical tool for the analysis of structural problems is investigated for solving plates with irregular domains. Using a four-nodded super element the physical domain is transformed into the computational domain. The thin plate governing equations can then be transformed using two second order transformations. Simply supported, clamped and free boundary conditions are considered.

2. Review of the GDQM

In the method of DQ the partial derivative of the field variable at the discrete point in the computational domain is approximated by a weighted linear sum of the values of the field variable along the line that passes through that point which is parallel to the coordinate direction of the derivative. Therefore, according to the differential quadrature rule for any function { }, one has

$$\left.\left\{\begin{array}{c}\dfrac{\partial\{\,\}}{\partial\xi}\\[2mm] \dfrac{\partial\{\,\}}{\partial\eta}\end{array}\right\}\right|_{(\xi_i,\eta_j)}=\left\{\begin{array}{c}\sum_{m=1}^{N_\xi} A_{im}^{(\xi)}\{\,\}_{mj}\\ \sum_{n=1}^{N_\eta} A_{jn}^{(\eta)}\{\,\}_{in}\end{array}\right\}, \tag{1}$$

$$\left.\left\{\begin{array}{c}\dfrac{\partial^2\{\,\}}{\partial\xi^2}\\[2mm] \dfrac{\partial^2\{\,\}}{\partial\eta^2}\\[2mm] \dfrac{\partial^2\{\,\}}{\partial\xi\partial\eta}\end{array}\right\}\right|_{(\xi_i,\eta_j)}=\left\{\begin{array}{c}\sum_{m=1}^{N_\xi} B_{im}^{(\xi)}\{\,\}_{mj}\\ \sum_{n=1}^{N_\eta} B_{jn}^{(\eta)}\{\,\}_{in}\\ \sum_{m=1}^{N_\xi}\sum_{n=1}^{N_\eta} A_{im}^{(\xi)}A_{jn}^{(\eta)}\{\,\}_{mn}\end{array}\right\}, \tag{2}$$

where $A_{ij}^{(\xi)}$, $A_{ij}^{(\eta)}$ are the weighting coefficients corresponding to first order derivatives, and $B_{ij}^{(\xi)}$ and $B_{ij}^{(\eta)}$ are the weighting coefficients corresponding to second order derivatives in ξ and η directions. N_ξ and N_η are the number of grid points along ξ and η axes, respectively.

From the above approximations, one can realize that determination of the weighting functions plays an important role in DQM analysis. Among the many methods that have been used to evaluate the weighting coefficients in differential quadrature methods, the method developed by Shu and Richard [22] claimed to be computationally more efficient and accurate, is employed in this work. The weighting coefficients of the first order derivatives are determined as

$$A_{ij}^{(\xi)}=\begin{cases}\dfrac{P(\xi_i)}{(\xi_i-\xi_j)P^{(1)}(\xi_j)} & \text{for } i\neq j,\ i,j=1,2,\ldots,N_\xi,\\ -\sum_{j=1\ i\neq j}^{N_\xi} A_{ij}^{(\xi)} & \text{for } i=j,\ i,j=1,2,\ldots,N_\xi,\end{cases} \tag{3}$$

where $P(\xi)$ and its derivative are defined as

$$P(\xi_i)=\prod_{j=1,\ j\neq i}^{N_\xi}(\xi_i-\xi_j),\quad P^{(1)}(\xi_i)=\prod_{j=1,\ j\neq i}^{N_\xi}(\xi_i-\xi_j).$$

In order to evaluate the weighting coefficients for higher order derivatives, a proposed recurrence formula may be employed. For second order derivatives this formula may be employed in the form of

$$B_{ij}^{(\xi)} = 2A_{ij}^{(\xi)}\left[A_{ii}^{(\xi)} - \frac{1}{(\xi_i - \xi_j)}\right] \quad \text{for } i,j = 1, 2, \ldots, N_\xi,\ i \neq j. \tag{4}$$

Another important point in DQM analysis is how to distribute the grid points. A natural, and the simplest, choice of the grid points through the computational domain is equally spaced points in the co-ordinate directions of the computational domain. It is demonstrated that non-uniform grid points usually yield better results than those of equally spaced points. The zeros of orthogonal polynomials are a rational basis for the grid points. Shu and Richards [22] have used other choices which have given a better result than the zeros of Chebyshev and Legendre [1]

$$(\xi_i, \eta_j) = \frac{1}{2}\left(\left[1 - \cos\frac{(i-1)\pi}{N_\xi - 1}\right], \left[1 - \cos\frac{(j-1)\pi}{N_\eta - 1}\right]\right). \tag{5}$$

3. The new methodology

A natural co-ordinate system (ξ, η) for the computational domain is chosen, where $-1 \leqslant \xi, \eta \leqslant 1$. The displacement w, and the second derivative of the displacement with respect to the natural coordinate variable normal to the boundary, and only along the boundary, would be set as the two degrees of freedom of the problem. For example along the boundary, $\xi = 0$, $\kappa^\xi = \partial^2 w/\partial\xi^2$ presents the second degree of freedom. Hence, in general, κ^n ($n = \xi$ or η) would play the role of an unknown parameter on the boundary. In order to incorporate the new degrees of freedom into differential equations and facilitate the boundary conditions implementation, the higher order derivatives (derivative with order $\geqslant 2$) with respect to the co-ordinate system of the actual domain would be expressed in terms of κ^n ($n = \xi$ or η) and also the displacement w using the geometrical mapping procedure.

4. Geometrical mapping

Consider an arbitrary straight-sided quadrilateral plate shown in Fig. 1(a). The geometry of this plate can be mapped into a rectangular plate to be referred as the computational domain. The coordinate axes of the quadrilateral plate which occupy the actual (or physical) domain are denoted by x, and y; whereas those of the computational domain are denoted by ξ, and η. The mapping process follows the standard procedure used widely in conventional finite element formulations; the physical domain is mapped into computational domain according to the following transformation law:

$$x = \sum_{i=1}^{N_s} x_i \psi_i(\xi, \eta), \quad y = \sum_{i=1}^{N_s} y_i \psi_i(\xi, \eta), \tag{6}$$

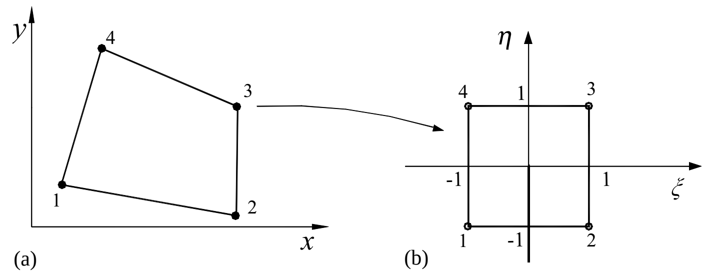

Fig. 1. (a) An arbitrary straight-sided quadrilateral plate (physical domain), (b) computational domain.

where x_i and y_i are the co-ordinates of node i in the physical domain, and N_s is the number of nodal points. $\psi_i(\xi,\eta)$ is the shape function associated with node i:

$$\psi_i(\xi,\eta) = \tfrac{1}{4}(1+\xi\xi_i)(1+\eta\eta_i), \quad i = 1,\dots,4, \tag{7}$$

where ξ_i and η_i are the coordinates of nodal point i in the computational domain $\xi - \eta$. The transformation law (7) will rule the relations between the geometry of the two domains. The derivatives of any function defined in one domain may be transformed into the other using the mapping or shape function rule defined. For example the first, second and third derivatives of any function $\{\,\}$ in the computational domain may be obtained in terms of the derivatives in the physical domain from the chain rule according to

$$\{\,\}_{,i} = \sum_{I=1}^{2} \{\,\}_{,I} x_{I,i}, \tag{8}$$

$$\{\,\}_{,ij} = \sum_{I=1}^{2} \{\,\}_{,I} x_{I,ij} + \sum_{I=1}^{2}\sum_{J=1}^{2} \{\,\}_{,IJ} x_{I,i} x_{J,j}, \tag{9}$$

$$\begin{aligned}\{\,\}_{,ijk} = {} & \sum_{I=1}^{2} \{\,\}_{,I} x_{I,ijk} + \sum_{I=1}^{2}\sum_{I=1}^{2} \{\,\}_{,IJ}(x_{I,ij}x_{J,k} + x_{I,ik}x_{J,j} + x_{I,i}x_{J,jk}) \\ & + \sum_{I=1}^{2}\sum_{J=1}^{2}\sum_{K=1}^{2} \{\,\}_{,IJK} x_{I,i} x_{J,j} x_{K,k},\end{aligned} \tag{10}$$

where $x_{I,i}$, $x_{I,ij}$ and $x_{I,ijk}$, the components of transformation matrices for derivatives, are related to the shape functions which map the geometry at the two co-ordinates. $x_{I,i}$ are the components of the so-called Jacobian transformation matrix. The inverse transformation matrices may be evaluated so that the derivatives in the physical domain may be determined in terms of the derivatives in the computational domain, so that

$$\left\{ \begin{array}{c} \dfrac{\partial\{\,\}}{\partial x} \\ \dfrac{\partial\{\,\}}{\partial y} \end{array} \right\} = [T_{11}] \left\{ \begin{array}{c} \dfrac{\partial\{\,\}}{\partial \xi} \\ \dfrac{\partial\{\,\}}{\partial \eta} \end{array} \right\}, \tag{11}$$

$$\begin{Bmatrix} \dfrac{\partial^2\{\,\}}{\partial x^2} \\ \dfrac{\partial^2\{\,\}}{\partial y^2} \\ \dfrac{\partial^2\{\,\}}{\partial x\partial y} \end{Bmatrix} = [T_{21}]\begin{Bmatrix} \dfrac{\partial\{\,\}}{\partial \xi} \\ \dfrac{\partial\{\,\}}{\partial \eta} \end{Bmatrix} + [T_{22}]\begin{Bmatrix} \dfrac{\partial^2\{\,\}}{\partial \xi^2} \\ \dfrac{\partial^2\{\,\}}{\partial \eta^2} \\ \dfrac{\partial^2\{\,\}}{\partial \xi\partial \eta} \end{Bmatrix}, \tag{12}$$

$$\begin{Bmatrix} \dfrac{\partial^3\{\,\}}{\partial x^3} \\ \dfrac{\partial^3\{\,\}}{\partial y^3} \\ \dfrac{\partial^3\{\,\}}{\partial x^2\partial y} \\ \dfrac{\partial^3\{\,\}}{\partial x\partial y^2} \end{Bmatrix} = [T_{31}]\begin{Bmatrix} \dfrac{\partial\{\,\}}{\partial \xi} \\ \dfrac{\partial\{\,\}}{\partial \eta} \end{Bmatrix} + [T_{32}]\begin{Bmatrix} \dfrac{\partial^2\{\,\}}{\partial \xi^2} \\ \dfrac{\partial^2\{\,\}}{\partial \eta^2} \\ \dfrac{\partial^2\{\,\}}{\partial \xi\partial \eta} \end{Bmatrix} + [T_{33}]\begin{Bmatrix} \dfrac{\partial^3\{\,\}}{\partial \xi^3} \\ \dfrac{\partial^3\{\,\}}{\partial \eta^3} \\ \dfrac{\partial^3\{\,\}}{\partial \xi^2\partial \eta} \\ \dfrac{\partial^3\{\,\}}{\partial \xi\partial \eta^2} \end{Bmatrix}, \tag{13}$$

where $[T_{ij}]$, the inverse transformation matrices, are related to the transformation matrices according to

$$[T_{11}] = [J_{11}]^{-1}, \quad [T_{21}] = -[J_{22}]^{-1}[J_{21}][J_{11}]^{-1}, \quad [T_{22}] = [J_{22}]^{-1},$$

$$[T_{31}] = -[J_{33}]^{-1}[J_{31}][J_{11}]^{-1}, \quad [T_{32}] = -[J_{33}]^{-1}[J_{32}][J_{22}]^{-1}, \quad [T_{33}] = [J_{33}]^{-1}.$$

In Appendix A, the components of the transformation matrices, $[J_{ij}]$, are cited.

Employing the transformation matrices, both the governing equation as well as the boundary conditions of the problem under consideration may be transformed from the physical to the computational domain and vice versa.

5. DQ analog of plate governing equation

For generality of the problem under consideration, the governing equation of a thin, materially and geometrically symmetric, elastic plate is considered as the governing equation, that is,

$$C_1\frac{\partial^4 w}{\partial x^4} + C_2\frac{\partial^4 w}{\partial x^3\partial y} + C_3\frac{\partial^4 w}{\partial x^2\partial y^2} + C_4\frac{\partial^4 w}{\partial x\partial y^3} + C_5\frac{\partial^4 w}{\partial y^4} - N_x\frac{\partial^2 w}{\partial x^2}$$
$$- N_y\frac{\partial^2 w}{\partial y^2} - 2N_{xy}\frac{\partial^2 w}{\partial x\partial y} + kw + \rho h\frac{\partial^2 w}{\partial t^2} = p(x,y,t), \tag{14}$$

where w, N_x, N_y, N_{xy}, and $p(x,y,t)$ are the transverse displacement, in plane normal and shear edge forces in x and y directions, and the intensity of transverse distributed loads respectively. Also, C_i, ρ, h, k are, respectively, the flexural rigidity coefficients, density, thickness, and elastic stiffness of the support.

Two second order transformation processes transform the governing equation from the physical domain into the computational domain. Bert and Malik [14] have used the first order transformation rule four times to do the job. The approach employed here will need less computational efforts. To employ the second order transformations, K^x and K^y are defined as

$$K^x = \frac{\partial^2 w}{\partial x^2}, \quad K^y = \frac{\partial^2 w}{\partial y^2}. \tag{15}$$

Using these definitions, the free vibration governing equation extracted from Eq. (14) takes the form

$$\{C_x\}^{\mathrm{T}} \begin{Bmatrix} \dfrac{\partial^2 K^x}{\partial x^2} \\ \dfrac{\partial^2 K^x}{\partial y^2} \\ \dfrac{\partial^2 K^x}{\partial x \partial y} \end{Bmatrix} + \{C_y\}^{\mathrm{T}} \begin{Bmatrix} \dfrac{\partial^2 K^y}{\partial x^2} \\ \dfrac{\partial^2 K^y}{\partial y^2} \\ \dfrac{\partial^2 K^y}{\partial x \partial y} \end{Bmatrix} + kw + \rho h \frac{\partial^2 w}{\partial t^2} = 0, \tag{16}$$

where

$$\{C_x\}^{\mathrm{T}} = [C_1 \quad \tfrac{1}{2}C_4 \quad C_3], \quad \{C_y\}^{\mathrm{T}} = [\tfrac{1}{2}C_4 \quad C_2 \quad C_5].$$

Employing the second order transformation law, given by Eq. (12), the free vibration governing equation (16) becomes

$$\begin{aligned} &\{C_x\}^{\mathrm{T}} \left([T_{22}] \begin{Bmatrix} \dfrac{\partial^2 K^x}{\partial \xi^2} \\ \dfrac{\partial^2 K^x}{\partial \eta^2} \\ \dfrac{\partial^2 K^x}{\partial \xi \partial \eta} \end{Bmatrix} + [T_{21}] \begin{Bmatrix} \dfrac{\partial K^x}{\partial \xi} \\ \dfrac{\partial K^x}{\partial \eta} \end{Bmatrix} \right) \\ &+ \{C_y\}^{\mathrm{T}} \left([T_{22}] \begin{Bmatrix} \dfrac{\partial^2 K^y}{\partial \xi^2} \\ \dfrac{\partial^2 K^y}{\partial \eta^2} \\ \dfrac{\partial^2 K^y}{\partial \xi \partial \eta} \end{Bmatrix} + [T_{21}] \begin{Bmatrix} \dfrac{\partial K^x}{\partial \xi} \\ \dfrac{\partial K^x}{\partial \eta} \end{Bmatrix} \right) + kw + \rho h \frac{\partial^2 w}{\partial t^2} = 0. \end{aligned} \tag{17}$$

If we set

$$\{\kappa\}^{\mathrm{T}} = \left[\frac{\partial^2 w}{\partial \xi^2} \quad \frac{\partial^2 w}{\partial \eta^2} \quad \frac{\partial^2 w}{\partial \xi \partial \eta} \right],$$

the second order derivatives are expressed in terms of displacement, w, for grid points within the domain, that is

$$\{\kappa\}|_{(\xi_i,\eta_j)} = \left\{ \begin{array}{c} \sum_{m=1}^{N_\xi} B_{im}^{(\xi)} w_{mj} \\ \sum_{n=1}^{N_\eta} B_{jn}^{(\eta)} w_{in} \\ \sum_{m=1}^{N_\xi} \sum_{n=1}^{N_\eta} A_{im}^{(\xi)} A_{jn}^{(\eta)} w_{mn} \end{array} \right\}$$

$$\text{for } i = 2, 3, \ldots, N_\xi - 1 \text{ and } j = 2, 3, \ldots, N_\eta - 1. \tag{18}$$

Using Eqs. (1), (2) and (18), the DQ analog of the plate free vibration may be written as

$$\sum_{m=1}^{N_\xi} \sum_{n=1}^{N_\eta} [H_{ijmn}^{(x)} \quad H_{ijmn}^{(y)}] \begin{bmatrix} K_{mn}^x \\ K_{mn}^y \end{bmatrix} + k w_{ij} + \rho h \frac{\partial^2 w_{ij}}{\partial t^2} = 0$$

$$\text{for } i = 2, 3, \ldots, N_\xi - 1 \text{ and } j = 2, 3, \ldots, N_\eta - 1, \tag{19}$$

where

$$H_{ijmn}^{(x)} = \{C_x\}^{\mathrm{T}} \left([T_{21}]_{ij} \left\{ \begin{array}{c} A_{im}^{(\xi)} \delta_{jn} \\ A_{jn}^{(\eta)} \delta_{im} \end{array} \right\} + [T_{22}]_{ij} \left\{ \begin{array}{c} B_{im}^{(\xi)} \delta_{jn} \\ B_{jn}^{(\eta)} \delta_{im} \\ A_{im}^{(\xi)} A_{jn}^{(\eta)} \end{array} \right\} \right),$$

$$H_{ijmn}^{(y)} = \{C_y\}^{\mathrm{T}} \left([T_{21}]_{ij} \left\{ \begin{array}{c} A_{im}^{(\xi)} \delta_{jn} \\ A_{jn}^{(\eta)} \delta_{im} \end{array} \right\} + [T_{22}]_{ij} \left\{ \begin{array}{c} B_{im}^{(\xi)} \delta_{jn} \\ B_{jn}^{(\eta)} \delta_{im} \\ A_{im}^{(\xi)} A_{jn}^{(\eta)} \end{array} \right\} \right)$$

$$\text{for } i = 2, 3, \ldots, N_\xi - 1 \text{ and } j = 2, 3, \ldots, N_\eta - 1.$$

A second order transformation will be used to transform K^x and K^y from the physical domain into the computational domain. To do so, one may employ Eq. (12) in the following form at any arbitrary grid point (ξ_m, η_n):

$$\left\{ \begin{array}{c} K^x \\ K^y \end{array} \right\}_{mn} = [\bar{T}_{21}]_{mn} \left\{ \begin{array}{c} \dfrac{\partial w}{\partial \xi} \\ \dfrac{\partial w}{\partial \eta} \end{array} \right\}_{mn} + [\bar{T}_{22}]_{mn} \left\{ \begin{array}{c} \dfrac{\partial^2 w}{\partial \xi^2} \\ \dfrac{\partial^2 w}{\partial \eta^2} \\ \dfrac{\partial^2 w}{\partial \xi \partial \eta} \end{array} \right\}_{mn}, \tag{20}$$

where $[\bar{T}_{21}]$ and $[\bar{T}_{22}]$ are the reduced form of the second order transformation $[T_{21}]$ and $[T_{22}]$. Employing the above relation, and assuming zero elastic coefficient for the supports, Eq. (19) may be written as

$$\sum_{m=1}^{N_\xi}\sum_{n=1}^{N_\eta}[H_{ijmn}^{(x)} \quad H_{ijmn}^{(y)}][\bar{T}_{21}]_{mn}\begin{Bmatrix}\dfrac{\partial w}{\partial \xi}\\ \dfrac{\partial w}{\partial \eta}\end{Bmatrix}_{mn} + \sum_{m=1}^{N_\xi}\sum_{n=1}^{N_\eta}[H_{ijmn}^{(x)} \quad H_{ijmn}^{(y)}][\bar{T}_{22}]_{mn}\begin{Bmatrix}\dfrac{\partial^2 w}{\partial \xi^2}\\ \dfrac{\partial^2 w}{\partial \eta^2}\\ \dfrac{\partial^2 w}{\partial \xi \partial \eta}\end{Bmatrix}_{mn}$$

$$+ \; kw_{ij} + \rho h\frac{\partial^2 w_{ij}}{\partial t^2} = 0 \quad \text{for } i = 2,3,\ldots,N_\xi - 1 \text{ and } j = 2,3,\ldots,N_\eta - 1. \tag{21}$$

Using the quadrature rule for first and second order derivatives (except for those which are chosen as the degree of freedom at the boundary points) one may reduce the governing equation to a standard form

$$[S_{db}]\{U_b\} + [S_{dd}]\{U_d\} + \rho h\left\{\frac{\partial^2 U_d}{\partial t^2}\right\} = \{0\}. \tag{22}$$

In the above equation,

$$\{U_b\} = \begin{Bmatrix}\{w\}_b\\ \{\kappa\}_b\end{Bmatrix}, \quad \{U_d\} = \{w\}_d.$$

The subscript b denotes a boundary point whereas d represents a domain grid point.

6. DQ boundary conditions implementation

In the following section DQ analogs of three types of classical boundary conditions, i.e., simply supported (S), clamped (C), and free edges (F) will be presented. In order to simplify the notations in the DQ analogs, we use the indices b_ξ for the edges $\xi = \pm 1$ which take the value of 1 at the edge $\xi = -1$ and N_ξ at the edge $\xi = 1$, respectively. Similarly, b_η will be used for the edges $\eta = \pm 1$, in which $b_\eta = 1$ at $\eta = -1$ and $b_\eta = N_\eta$, at the edge $\eta = 1$, respectively.

6.1. Simply supported boundary conditions

For simply supported edges, the boundary conditions are

$$w = 0, \quad M_n = 0. \tag{23}$$

The bending moment M_n can be expressed in terms of the Cartesian components of the moments at that point as [23]

$$M_n = n_x^2 M_x + n_y^2 M_y + 2n_x n_y M_{xy},$$

where n_x and n_y are, respectively, the x and y components of unit normal to the boundary. Eq. (23) may be formatted as

$$M_n = \{\bar{n}\}^{\mathrm{T}}\{M\} = \{\bar{n}\}^{\mathrm{T}}[\bar{D}]\{K\}, \tag{24}$$

where

$$\{\bar{n}\}^{\mathrm{T}} = \{n_x^2 \quad n_y^2 \quad 2n_x n_y\}, \quad [\bar{D}] = [\bar{I}][D], \quad [\bar{I}] = \begin{bmatrix} 1 & 0 & 0 \\ 0 & 1 & 0 \\ 0 & 0 & 2 \end{bmatrix}.$$

$[D]$ is the bending stiffness matrix of the plate (see Appendix B). Using the second order transformation law (12), Eq. (24) reads

$$\{\bar{M}_1\}^{\mathrm{T}} \begin{Bmatrix} \dfrac{\partial w}{\partial \xi} \\ \dfrac{\partial w}{\partial \eta} \end{Bmatrix} + \{\bar{M}_2\}^{\mathrm{T}} \begin{Bmatrix} \dfrac{\partial^2 w}{\partial \xi^2} \\ \dfrac{\partial^2 w}{\partial \eta^2} \\ \dfrac{\partial^2 w}{\partial \xi \partial \eta} \end{Bmatrix} = 0, \tag{25}$$

where

$$\{\bar{M}_1\}^{\mathrm{T}} = \{\bar{n}\}^{\mathrm{T}}[\bar{D}][T_{21}], \quad \{\bar{M}_2\}^{\mathrm{T}} = \{\bar{n}\}^{\mathrm{T}}[\bar{D}][T_{22}].$$

If edges $\xi = -1$ or $\xi = 1$ are simply supported, the DQ analog of the first equation (23) will take the form of

$$w_{b_\xi J} = 0, \quad \text{for } J = 2, 3, \ldots, N_\eta - 1 \text{ and } b_\xi = 1 \text{ or } b_\xi = N_\xi, \tag{26}$$

whereas, the DQ analog of the second equation (23) is

$$\{\bar{M}_1\}^{\mathrm{T}}_{b_\xi J} \begin{Bmatrix} \sum_{m=1}^{N_\xi} A^{(\xi)}_{b_\xi m} w_{mJ} \\ \sum_{n=1}^{N_\eta} A^{(\eta)}_{Jn} w_{b_\xi n} \end{Bmatrix} + \{\bar{M}_2\}^{\mathrm{T}}_{b_\xi J} \begin{Bmatrix} \kappa^{\xi}_{b_\xi J} \\ \sum_{n=1}^{N_\eta} B^{(\eta)}_{Jn} w_{b_\xi n} \\ \sum_{m=1}^{N_\xi} \sum_{n=1}^{N_\eta} A^{(\xi)}_{b_\xi m} A^{(\eta)}_{Jn} w_{mn} \end{Bmatrix} = 0. \tag{27}$$

In the same way for edges $\eta = -1$ or $\eta = 1$:

$$w_{Ib_\eta} = 0, \quad \text{for } I = 2, 3, \ldots, N_\xi - 1 \text{ and } b_\eta = 1 \text{ or } b_\eta = N_\eta, \tag{28}$$

$$\{\bar{M}_1\}^{\mathrm{T}}_{Ib_\eta} \begin{Bmatrix} \sum_{m=1}^{N_\xi} A^{(\xi)}_{Im} w_{mb_\eta} \\ \sum_{n=1}^{N_\eta} A^{(\eta)}_{b_\eta n} w_{In} \end{Bmatrix} + \{\bar{M}_2\}^{\mathrm{T}}_{Ib_\eta} \begin{Bmatrix} \sum_{n=1}^{N_\eta} B^{(\eta)}_{Im} w_{mb_\eta} \\ \kappa^{\eta}_{Ib_\eta} \\ \sum_{m=1}^{N_\xi} \sum_{n=1}^{N_\eta} A^{(\xi)}_{Im} A^{(\eta)}_{b_\eta n} w_{mn} \end{Bmatrix} = 0. \tag{29}$$

6.2. Clamped boundary conditions

The boundary conditions for clamped edges can be stated as

$$w = 0, \quad \frac{\partial w}{\partial n} = 0, \tag{30}$$

where n stands for ξ and η.

If the edges $\xi = -1$ or $\xi = 1$ are clamped, the DQ analog of the first equation in (30) becomes

$$w_{b_\xi J} = 0, \quad \text{for } J = 2, 3, \ldots, N_\eta - 1 \text{ and } b_\xi = 1 \text{ or } b_\xi = N_\xi. \tag{31}$$

Zero slope boundary condition are implemented through κ^ξ. For example, along the edge $\xi = -1$ the condition $\partial w/\partial\xi = 0$ might be implemented by

$$\kappa^\xi_{b_\xi J} - \sum_{M=ml}^{mu} A^{(\xi)}_{b_\xi M} \left.\frac{\partial w}{\partial \xi}\right|_{(\xi_M, \eta_J)} = 0, \quad \text{for } J = 2, 3, \ldots, N_\eta - 1, \tag{32}$$

where $ml = 2$ for the zero slope condition at $\xi = -1$, otherwise $ml = 1$. For zero slope condition at edge $\xi = 1$, $mu = N_\xi - 1$, otherwise, $mu = N_\xi$. Also as stated before, $b_\xi = 1$ for $\xi = -1$ and $b_\xi = N_\xi$ for $\xi = 1$. The slope term in the summation in Eq. (32) can be expanded

$$\kappa^\xi_{b_\xi J} - \sum_{M=ml}^{mu} \sum_{n=1}^{N_\xi} A^{(\xi)}_{b_\xi M} A^{(\xi)}_{Mn} w_{nJ} = 0, \quad \text{for } J = 2, 3, \ldots, N_\eta - 1. \tag{33}$$

In a similar way, one can implement the clamped boundary condition at edge $\eta = -1$ or $\eta = 1$; the results read

$$w_{Ib_\eta} = 0, \quad \text{for } I = 2, 3, \ldots, N_\xi - 1 \text{ and } b_\eta = 1 \text{ or } b_\eta = N_\eta, \tag{34}$$

$$\kappa^\eta_{Ib_\eta} - \sum_{M=ml}^{mu} \sum_{n=1}^{N_\eta} A^{(\eta)}_{b_\eta M} A^{(\eta)}_{Mn} w_{In} = 0, \quad \text{for } I = 2, 3, \ldots, N_\xi - 1, \tag{35}$$

where $ml = 2$ if a zero slope condition applies to the edge $\eta = -1$, otherwise, $ml = 1$. For zero slope condition at edge $\eta = 1$, $mu = N_\eta - 1$, otherwise $mu = N_\eta$. Also, $b_\eta = 1$ for $\eta = -1$ and $b_\eta = N_\eta$ for $\eta = 1$.

6.3. Free-edge boundary condition

For the free boundary conditions [23]

$$M_n = 0, \quad Q_n + \frac{\partial M_{sn}}{\partial s} = 0 \tag{36}$$

should be satisfied. s, and n are the coordinate variables of the axes tangent and normal to the boundary, Q_n is the shear force, and M_{sn} is the twisting moment at the edges [23]. The DQ analog of M_n is given by Eqs. (27) and (29). The DQ analogs of the effective shear stresses are derived here based on a new approach [12]. In order to do so, Eq. (36) may be written as

$$\{F\}^{\mathrm{T}}\begin{Bmatrix}\dfrac{\partial^3 w}{\partial x^3}\\ \dfrac{\partial^3 w}{\partial y^3}\\ \dfrac{\partial^3 w}{\partial x^2\partial y}\\ \dfrac{\partial^3 w}{\partial x\partial y^2}\end{Bmatrix}=0. \tag{37}$$

The details of derivation and also the definition of matrix $\{F\}$ are given in Appendix B. Using Eqs. (13), Eq. (37) becomes

$$\{\bar{F}_3\}^{\mathrm{T}}\begin{Bmatrix}\dfrac{\partial^3 w}{\partial \xi^3}\\ \dfrac{\partial^3 w}{\partial \eta^3}\\ \dfrac{\partial^3 w}{\partial \xi^2\partial \eta}\\ \dfrac{\partial^3 w}{\partial \xi\partial \eta^2}\end{Bmatrix}+\{\bar{F}_2\}^{\mathrm{T}}\begin{Bmatrix}\dfrac{\partial^2 w}{\partial \xi^2}\\ \dfrac{\partial^2 w}{\partial \eta^2}\\ \dfrac{\partial^2 w}{\partial \xi\partial \eta}\end{Bmatrix}+\{\bar{F}_1\}^{\mathrm{T}}\begin{Bmatrix}\dfrac{\partial w}{\partial \xi}\\ \dfrac{\partial w}{\partial \eta}\end{Bmatrix}=0, \tag{38}$$

where

$$\{\bar{F}_3\}=\{F\}^{\mathrm{T}}[T_{33}],\quad \{\bar{F}_2\}=\{F\}^{\mathrm{T}}[T_{32}],\quad \{\bar{F}_1\}=\{F\}^{\mathrm{T}}[T_{31}].$$

Along the edges $\xi=-1$ or $\xi=1$, the differential quadrature rule can be applied to Eq. (38) to derive DQ analogs of zero effective shear forces

$$\begin{aligned}&\{\bar{F}_3\}^{\mathrm{T}}_{b_\xi J}\begin{Bmatrix}\sum_{m=1}^{N_\xi} C^{(\xi)}_{b_\xi m} w_{mJ}\\ \sum_{n=1}^{N_\xi} C^{(\xi)}_{jn} w_{b_\xi n}\\ \sum_{m=1}^{N_\xi}\sum_{n=1}^{N_\eta} B^{(\xi)}_{b_\xi m} A^{(\xi)}_{Jn} w_{mn}\\ \sum_{m=1}^{N_\xi}\sum_{n=1}^{N_\eta} A^{(\xi)}_{b_\xi m} B^{(\xi)}_{Jn} w_{mn}\end{Bmatrix}+\{\bar{F}_2\}^{\mathrm{T}}_{b_\xi J}\begin{Bmatrix}\kappa^{\xi}_{b_\xi J}\\ \sum_{n=1}^{N_\xi} B^{(\xi)}_{jn} w_{b_\xi n}\\ \sum_{m=1}^{N_\xi}\sum_{n=1}^{N_\eta} A^{(\xi)}_{b_\xi m} A^{(\xi)}_{Jn} w_{mn}\end{Bmatrix}\\ &+\{\bar{F}_1\}^{\mathrm{T}}_{b_\xi J}\begin{Bmatrix}\sum_{m=1}^{N_\xi} A^{(\xi)}_{b_\xi m} w_{mJ}\\ \sum_{n=1}^{N_\xi} A^{(\xi)}_{b_\xi n} w_{b_\xi n}\end{Bmatrix}=0,\quad \text{for } J=2,3,\ldots,N_\eta-1.\end{aligned} \tag{39}$$

The above relations along the edges $\eta = -1$ or $\eta = 1$ can be written similarly

$$\{\bar{F}_3\}^{\mathrm{T}}_{Ib_\eta}\left\{\begin{array}{c}\sum_{m=1}^{N_\xi} C^{(\eta)}_{Im} w_{mb_\eta}\\ \sum_{n=1}^{N_\eta} C^{(\eta)}_{b_\eta n} w_{In}\\ \sum_{m=1}^{N_\xi}\sum_{n=1}^{N_\eta} B^{(\eta)}_{Im} A^{(\eta)}_{b_\eta n} w_{mn}\\ \sum_{m=1}^{N_\xi}\sum_{n=1}^{N_\eta} A^{(\eta)}_{Im} B^{(\eta)}_{b_\eta n} w_{mn}\end{array}\right\} + \{\bar{F}_2\}^{\mathrm{T}}_{Ib_\eta}\left\{\begin{array}{c}\sum_{n=1}^{N_\xi} B^{(\eta)}_{Im} w_{mb_\eta}\\ \kappa^{\eta}_{Ib_\eta}\\ \sum_{m=1}^{N_\xi}\sum_{n=1}^{N_\eta} A^{(\eta)}_{Im} A^{(\eta)}_{b_\eta n} w_{mn}\end{array}\right\}$$

$$+\ \{\bar{F}_1\}^{\mathrm{T}}_{Ib_\eta}\left\{\begin{array}{c}\sum_{m=1}^{N_\xi} A^{(\eta)}_{Im} w_{mb_\eta}\\ \sum_{n=1}^{N_\eta} A^{(\eta)}_{b_\eta n} w_{In}\end{array}\right\} = 0, \quad \text{for } I = 2, 3, \ldots, N_\xi - 1. \tag{40}$$

7. The assembled system of equations

The free vibration assembled form of the analogue equations (22) becomes

$$[S_{db}]\{U_b\} + [S_{dd}]\{U_d\} - \rho h\omega^2\{U_d\} = \{0\}, \tag{41}$$

where ω is the natural frequency of the plate. The boundary conditions may also be rearranged to the following form:

$$[S_{bb}]\{U_b\} + [S_{bd}]\{U_d\} = \{0\}. \tag{42}$$

By eliminating the boundary degrees of freedom from the system of Eq. (41), one obtains a standard eigenvalue problem

$$([S] - \rho\omega^2[I])\{U_d\} = \{0\}, \tag{43}$$

where $[S] = [S_{dd}] - [S_{db}][S_{bb}]^{-1}[S_{bd}]$. $[I]$ is the identity matrix of order $(N_x - 2) \times (N_y - 2)$. From Eq. (43), one can perform the eigenvalue analysis of a matrix of order $(N_x - 2) \times (N_y - 2)$ to obtain the natural frequencies as well as the mode shapes of the system under consideration.

8. Numerical results

In order to demonstrate the efficiency of the methodology for the free vibration analysis of irregular straight-sided quadrilateral plates, many different cases were studied. Free vibration problems of skew plates (see Fig. 2) with different boundary conditions and with different aspect ratios (a/b) and skew angles (θ) are studied first, followed by the analysis of trapezoidal plates under different configurations.

In the examples considered, each plate will be identified by Leissa's [24] convention; for examples, the symbolism C–S–C–F indicates that the left edge, is clamped, right edge is simply supported, lower edge is clamped and upper edges are free, respectively. The Poisson ratio is 0.3 for all the examples considered. Applications of the method to static and stability analysis of skew and irregular straight-sided plate problems are demonstrated elsewhere [25].

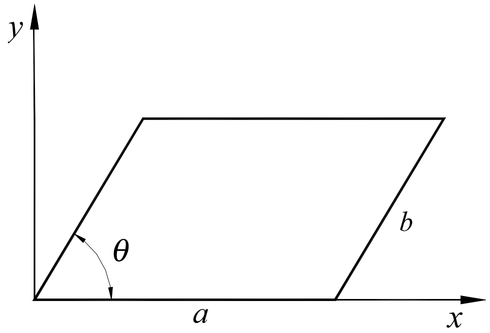

Fig. 2. Geometry of a skew plate.

8.1. Skew plates

In Table 1, the first five non-dimensional frequencies ($\bar{\omega} = \omega a^2 \sqrt{\rho h/D}$) of simply supported skew plates for three different aspect ratios and for an acute skew angle of 30° are presented. The results obtained by the present method are compared with those obtained by the hierarchical finite element method (HFEM), claimed to be the most accurate numerical method for solving eigenvalue problems in structural analysis [26]. Also, comparisons were made with some other available results from other methods [27]. As it is evident from this table, in the present DQ analysis, the fundamental frequencies can be obtained accurately with only five grid points in each direction of the computational co-ordinate axes, needing an eigenvalue analysis of a matrix of order nine only. The results obtained by the present methodology have closer agreement with HFEM [26] than those of Singh and Chakraverty [27].

In Table 2, the first five non-dimensional frequencies of a clamped plate with an acute skew angle of 30° for three aspect ratios are presented. Also, the results for a plate with C–C–S–S boundary conditions and a skew angle of 30° are given in Table 3. In all cases, for every aspect ratio and every skew angle, excellent agreements with HFEM [26] results are achieved. The results are also compared with those of Singh and Chakravarty and also MacGee et al. [28].

In Table 4, the results for the first five non-dimensional frequencies of rhombic plates with S–C–S–C boundary conditions are presented for three different numbers of grid points in each direction at different skew angles. This example has also been studied by MacGee et al. [28]. In their study, they have considered the effects of stress singularities at the corners for rhombic plates on simply supported or clamped boundary conditions. The agreement between the present method results and those of Refs. [28,24,29] is excellent. Once can conclude that by the present DQ methodology, only seven grid points in each directions suffice to yield an accurate solution.

In Table 5 the convergence behavior of the first five natural frequencies of a S–F–S–F rhombic plate for two different skew angles are studied. It is for the first time that DQ analysis results for thin skew plate with free edges are presented. Convergence, stability, and accuracy of the results are satisfied for such boundary conditions. Again close agreement with those of references [26,27,30] can be seen. In Table 6, the results of skew plate analysis with C–F–C–F boundary conditions at different skew angles are considered. In the previous results it was evident that the present methodology results have a better accuracy than previous DQ methods in the cases where

Table 1
Convergence of natural frequencies of simply supported skew plates (skew angle = 30°)

Aspect ratio	Method	N_ξ	Mode sequence				
			1	2	3	4	5
$a/b=2$	Present	5	188.0468	311.4303	461.9595	831.3994	1039.1471
		7	176.4545	229.2691	323.8561	599.2835	717.5473
		9	175.1948	221.9028	291.0736	403.5683	580.2583
		11	174.6661	220.6491	287.6053	371.9915	479.6142
		13	174.3636	219.9651	287.0794	369.1073	461.8238
		15	174.1574	219.4907	286.7384	369.0148	460.3482
		19	173.8898	218.8604	286.2543	368.9211	460.2766
		25	173.6591	218.3096	285.8122	368.8237	460.2470
	HFEM [26]		174.855	221.200	288.419	369.516	460.342
	Ref. [27]		182.44	240.11	394.64	562.85	675.53
$a/b=1$	Present	5	76.6428	160.3127	294.6147	316.3675	352.0000
		7	67.8490	108.5521	171.2030	223.8263	273.9755
		9	65.9436	105.0558	150.4475	203.9684	214.6864
		11	65.1742	104.9552	148.5354	196.6715	212.0060
		13	64.7119	104.9545	148.3134	196.2940	210.7962
		15	64.3917	104.9545	148.2111	196.2928	210.0440
		19	63.9717	104.9545	148.0877	196.2926	209.1020
		25	63.6082	104.9545	147.9860	196.2926	208.3130
	HFEM [26]		64.818	104.955	148.320	196.294	210.658
	Ref. [27]		73.135	112.64	209.84	233.52	323.51
$a/b=0.5$	Present	5	47.0117	77.8576	115.4899	207.8499	259.7868
		7	44.1136	57.3173	80.9640	149.8209	165.7619
		9	43.7987	55.4757	72.7684	100.8920	145.0646
		11	43.6665	55.1623	71.9013	92.9979	119.9035
		13	43.5909	54.9913	71.7698	92.2768	115.4560
		15	43.5394	54.8723	71.6845	92.2537	115.0871
		17	43.5015	54.7839	71.6172	92.2409	115.0738
		19	43.4724	54.7151	71.5636	92.2303	115.0691
		25	43.4148	54.5774	71.4530	92.2105	115.0617
	HFEM [26]		43.714	55.300	72.105	92.379	115.086

comparisons are made. This conclusion comes from the fact that the results given by Singh and Chakraverty [27] provide an upper bound to the fundamental natural frequencies as they have used the Rayleigh–Ritz method. In all cases the present method solutions converge to values less than those given by Singh and Chakraverty which is an indication of the accurate nature of the results. In Table 7, the results for the first five normalized natural frequencies of rhombic plates for different mixed boundary conditions and also for different skew angles are given. In all cases the present methodology fundamental frequencies are close, however, they are less than those given by Singh and Chakraverty [27]. These results are also compared with those of McGee et al. [28].

Table 2
Convergence of natural frequencies of skew plates with C–C–C–C edges (skew angle = 30°)

a/b	Method	N_ξ	Mode sequence				
			1	2	3	4	5
$a/b=2$	Present	7	189.2310	227.757	295.2616	515.1862	561.5448
		9	189.1715	221.7124	279.5416	415.8022	504.9571
		11	189.2931	222.3759	280.2522	359.1811	459.9340
		13	189.2931	222.4113	280.2492	359.5580	448.9228
		15	189.2940	222.4018	280.2446	358.9282	448.6766
		17	189.2940	222.4016	280.2472	358.9780	448.5197
		19	189.2940	222.4023	280.2477	358.9759	448.5375
	HFEM [26]		189.295	222.405	280.252	358.979	448.536
	Ref. [27]		190.00	223.98	294.67	385.53	509.03
$a/b=1.0$	Present	7	125.5083	214.7129	308.3456	332.6158	383.0270
		9	121.9704	180.0774	254.1165	312.0186	372.2743
		11	121.7864	177.7508	230.7331	292.1753	306.0871
		13	121.6800	177.7270	232.0490	292.4008	305.1902
		15	121.6622	177.7220	231.7400	291.4484	304.8950
		17	121.6514	177.7211	231.7554	291.5280	304.8280
		19	121.6462	177.7210	231.7510	291.5216	304.7966
	HFEM [26]		121.647	177.721	231.751	291.522	304.805
	B-spline [30]		120.903	177.752	231.738	292.535	301.813
	Ref. [27]		127.06	185.00	282.94	322.61	385.49
$a/b=0.5$	Present	7	47.3077	56.9392	73.8154	128.7965	140.3862
		9	47.2929	55.4281	69.8854	103.9505	126.240
		11	47.3232	55.5940	70.0630	89.7953	114.9835
		13	47.3233	55.6028	70.0623	89.8895	112.2307
		15	47.3235	55.6004	70.0611	89.7320	112.1691
		17	47.3235	55.6003	70.0618	89.7445	112.1300
		19	47.3235	55.6006	70.0619	89.7440	112.1344
	HFEM [26]		47.324	55.601	70.063	89.745	112.134

8.2. *Trapezoidal plates*

In Table 8, the first five natural frequencies ($\bar{\omega}=\omega a^2/\pi^2\sqrt{\rho h/D}$) of the trapezoidal plates (see Fig. 3) for two cases of S–S–S–S and C–C–C–C boundary conditions are given. The convergence, stability and accuracy were studied. It is evident that the convergence behavior of the present solution procedure for the case of a simply supported plate is better than that of the δ method used by Bert and Malik [14] and Wang et al. [32]. These results are compared with the solutions given by Liew and Lim [35]. One can conclude that 9 grid points in each direction are enough for an accurate solution.

For two aspect ratios of $a/b=\frac{2}{3}$ and $\frac{1}{2}$ and using a different number of grid points, the results for the first eight natural frequencies $\bar{\omega}=\omega a^2/2\pi\sqrt{\rho h/D})$ are shown in Table 9 which are compared with results by Chopra and Durvasula [36,37] and also Liew et al. [34]. Also, the

Table 3
Convergence of natural frequencies of C–C–S–S skew plates (skew angle = 30°)

a/b	Method	N_ξ	Mode sequence				
			1	2	3	4	5
$a/b = 0.5$		7	64.5588	77.1950	108.8681	189.7991	214.5942
		11	64.3221	73.8467	91.0157	115.7983	151.3288
		13	64.2964	73.7500	90.8780	114.0231	140.5973
		15	64.2788	73.7130	90.8250	113.8599	139.6482
		19	64.2628	73.6774	90.7853	113.8390	139.5532
	HFEM [26]		64.321	73.805	90.938	113.96	139.618
$a/b = 1$		7	86.0954	153.2025	239.0663	263.7736	330.2577
		11	84.5310	138.5284	186.6152	241.3483	246.3966
		13	84.4875	138.4656	186.7352	241.6146	245.8892
		15	84.4684	138.4659	186.7016	241.3344	245.7381
		19	84.4492	138.4602	186.6985	241.3500	245.6440
	HFEM [26]		84.669	138.529	186.739	241.393	246.352
	Ref. [28]		89.480	138.77	189.61	246.58	254.44
	Ref. [27]		92.906	151.39	221.70	278.46	407.42
$a/b = 2$		7	258.2353	308.7802	435.4725	759.1967	858.3768
		9	257.5178	295.5524	372.2196	532.5114	769.1081
		11	257.2885	295.3868	364.0626	463.1931	605.3153
		13	257.1854	294.9983	363.5116	456.0926	562.3891
		15	257.1154	294.8519	363.3001	455.4395	558.5926
		19	257.0511	294.7095	363.1411	455.3557	558.2127
	HFEM [26]		257.282	295.220	363.754	455.841	558.472
	Ref. [27]		262.94	322.02	422.83	751.71	839.39

solutions for trapezoidal plates when changing other geometrical parameters are studied. For a specific aspect ratio of $\frac{3}{2}$, the first eight natural frequencies are evaluated and presented in Table 10 for simply supported unsymmetrical trapezoidal plates with two different values of β as shown in Fig. 3. For two different values of cord ratios the first five natural frequencies of the trapezoidal plate are also presented in Table 11. Finally, natural frequencies for fixed aspect and cord ratios, and $\beta = 0$ under two different boundary conditions of S–C–S–C and S–C–S–F are presented in Table 12. Comparison of these results with those of Liew and Lam [38], Liew and Lam [35], Liew et al. [34] and Kuttler and Sigillito [39] certify the accuracy as well as the convergent behavior of the present methodology.

9. Conclusion

An efficient methodology is introduced to study the free vibration analysis of the irregular quadrilateral straight-sided thin plates. This methodology needs less computational efforts for

Table 4
Convergence of natural frequencies of S–C–S–C rhombic plate

Skew angle	Method	N_ξ	Mode sequence				
			1	2	3	4	5
90°	Present	11	28.95081	54.74243	69.3352	94.5820	102.20982
		15	28.95085	54.74307	69.3270	94.5853	102.21618
		19	28.95085	54.74307	69.3270	94.5853	102.21620
	Ref. [24]		28.951	54.743	69.327	94.585	102.22
75°	Present	11	30.6962	56.7013	74.6305	94.0545	111.9905
		15	30.6967	56.7027	74.6204	94.0464	111.9934
		19	30.6967	56.7028	74.6205	94.0464	111.9937
	Ref. [28]		30.697	56.703	74.621	94.046	111.99
	Ref. [29][a]		30.696	56.703	74.620	94.044	111.99
60°	Present	11	36.9500	64.2642	92.9795	100.8036	137.6825
		15	36.9529	64.2632	92.9690	100.7770	137.6797
		19	36.9534	64.2635	92.9708	100.7772	137.6814
	Ref. [28]		36.954	64.264	92.972	100.78	137.68
	Ref. [29][a]		36.963	64.270	93.004	100.78	137.71
	Ref. [27]		37.193	64.390	93.626	103.46	144.11
45°	Present	11	52.3640	83.5522	123.2821	136.9723	167.7025
		15	52.3716	83.5402	123.2464	136.9496	167.9604
		19	52.3737	83.5406	123.2472	136.9556	167.9625
	Ref. [28]		52.375	83.541	123.25	136.96	167.96
	Ref. [29][a]		52.489	83.596	123.28	137.35	167.96
	Ref. [27]		53.840	85.087	136.01	141.90	199.79
30°	Present	11	96.3540	137.2937	187.8254	237.9525	267.7209
		15	96.2521	137.2423	188.1137	237.7599	267.9262
		19	96.2274	137.2345	188.1094	237.7545	267.8761
	Ref. [28]		96.209	137.23	188.11	237.76	267.82
	Ref. [29][a]		97.272	137.53	188.41	238.76	270.44
	Ref. [27]		104.53	151.39	248.26	286.66	368.22

[a] $h/a = 0.01$.

evaluation of the weighting coefficients in comparison with other developed DQ procedures for fourth order partial differential equations. The physical domain is transformed to the computational domain by using a four-nodded super element. The governing equation and its related boundary conditions are transformed using the second and third order transformations in an efficient manner. The accuracy, convergence and stability of the solution procedure results are studied through different examples of the free vibration of irregular skew plates at acute angles under different boundary conditions, including the free-edge boundary type. The results are compared with those of other DQ methods as well as other numerical techniques. Excellent to very good agreements are achieved with the most accurate solutions.

Table 5
Convergence of natural frequencies of S–F–S–F rhombic plate

θ	Method	N_ξ	Mode sequence			
			1	2	3	4
60°	Present	5	12.7555	18.6067	35.5891	64.6762
		7	12.3762	18.0596	36.4753	50.7278
		9	12.2759	17.9157	36.0137	49.8634
		11	12.2390	17.8577	35.9991	49.6716
		13	12.2177	17.8184	35.9983	49.6027
		15	12.2031	17.7898	35.9991	49.5632
		17	12.1922	17.7686	35.9994	49.5354
		19	12.1840	17.7524	35.9993	49.5149
	HFEM [26]		12.147	17.703	36.026	49.394
	Ref. [27]		12.246	17.875	36.424	50.352
45°	Present	5	18.8710	23.2885	40.8290	91.9910
		7	16.8758	21.0548	39.5897	59.9930
		9	16.9528	21.17820	39.5575	59.8800
		11	16.8758	21.0548	39.5897	59.9930
		13	16.8089	20.9348	39.6017	59.9655
		15	16.7470	20.8382	39.6031	59.9160
		17	16.6938	20.7641	39.5985	59.8691
		19	16.6490	20.7068	39.5900	59.8317
	HFEM [26]		16.396	20.36	39.646	59.624
	B-spline [30]		16.413	20.41	39.646	59.672
	Ref. [27]		17.151	21.352	40.438	63.327

Appendix A. Transformation matrices

The transformation matrices are obtained from Eq. (8) as

$$[J_{11}] = \begin{bmatrix} x_{,\xi} & y_{,\xi} \\ x_{,\eta} & y_{,\eta} \end{bmatrix}, \quad [J_{21}] = \begin{bmatrix} x_{,\xi\xi} & y_{,\xi\xi} \\ x_{,\eta\eta} & y_{,\eta\eta} \\ x_{,\xi\eta} & y_{,\xi\eta} \end{bmatrix}, \tag{A.1}$$

$$[J_{22}] = \begin{bmatrix} x_{,\xi}^2 & y_{,\xi}^2 & x_{,\xi}y_{,\xi} \\ x_{,\eta}^2 & y_{,\eta}^2 & x_{,\eta}y_{,\eta} \\ x_{,\xi}x_{,\eta} & y_{,\xi}y_{,\eta} & \frac{1}{2}(x_{,\xi}y_{,\eta} + x_{,\eta}y_{,\xi}) \end{bmatrix}, \quad [J_{31}] = \begin{bmatrix} x_{,\xi\xi\xi} & y_{,\xi\xi\xi} \\ x_{,\eta\eta\eta} & y_{,\eta\eta\eta} \\ x_{,\xi\xi\eta} & y_{,\xi\xi\eta} \\ x_{,\xi\eta\eta} & y_{,\xi\eta\eta} \end{bmatrix}, \tag{A.2, A.3}$$

Table 6
Convergence of natural frequencies of C–F–C–F rhombic plate

θ	Method	N_ξ	Mode sequence				
			1	2	3	4	5
75°	Present	7	23.330	27.3702	44.9750	68.3494	73.7784
		11	23.3680	27.3877	44.8514	64.5387	70.4256
		15	23.3503	27.3431	44.8409	64.5023	70.3795
		17	23.3467	27.3362	44.8361	64.4962	70.3684
		19	23.3450	27.3320	44.8324	64.4922	70.3607
60°	Present	7	27.9905	30.9161	49.8745	73.5866	81.05646
		11	27.1323	30.5465	49.4217	74.5253	81.1313
		15	27.4272	30.6394	49.477	74.1159	81.107
		17	27.4216	30.6174	49.4798	74.0570	81.0607
		19	27.4146	30.5992	49.4806	74.0171	81.0223
	Ref. [27]		27.606	30.933	50.391	74.899	85.538
45°	Present	7	37.5985	39.4970	65.8802	102.080	111.1700
		11	37.1758	38.8394	62.1020	88.0291	103.4123
		15	36.7910	38.5093	61.8014	87.4642	102.9012
		17	36.6943	38.4079	61.7511	87.3112	102.7415
		19	36.6307	38.3336	61.7231	87.2013	102.6320
	Ref. [27]		38.338	40.209	63.695	91.941	119.97

$$[J_{32}] = \begin{bmatrix} 3x_{,\xi}x_{,\xi\xi} & 3y_{,\xi}y_{,\xi\xi} & 3(x_{,\xi\xi}y_{,\xi} + y_{,\xi\xi}x_{,\xi}) \\ 3x_{,\eta}x_{,\eta\eta} & 3y_{,\eta}y_{,\eta\eta} & 3(x_{,\eta\eta}y_{,\eta} + y_{,\eta\eta}x_{,\eta}) \\ x_{,\xi\xi}x_{,\eta} + 2x_{,\xi\eta}x_{,\xi} & y_{,\xi\xi}y_{,\eta} + 2y_{,\xi\eta}y_{,\xi} & x_{,\xi\xi}y_{,\eta} + y_{,\xi\xi}x_{,\eta} + 2x_{,\xi\eta}y_{,\eta} + 2y_{,\xi\eta}x_{,\xi} \\ x_{,\eta\eta}x_{,\xi} + 2x_{,\xi\eta}x_{,\eta} & y_{,\xi\xi}y_{,\xi} + 2y_{,\xi\eta}y_{,\eta} & x_{,\xi\xi}y_{,\eta} + y_{,\xi\xi}x_{,\eta} + 2x_{,\xi\eta}y_{,\eta} + 2y_{,\xi\eta}x_{,\xi} \end{bmatrix}, \tag{A.4}$$

$$[J_{33}] = \begin{bmatrix} x_{,\xi}^3 & y_{,\xi}^3 & 3x_{,\xi}^2y_{,\xi} & 3x_{,\xi}y_{,\xi}^2 \\ x_{,\eta}^3 & y_{,\eta}^3 & 3x_{,\eta}^2y_{,\eta} & 3x_{,\eta}y_{,\eta}^2 \\ x_{,\xi}^2x_{,\eta} & y_{,\xi}^2y_{,\eta} & x_{,\xi}^2y_{,\eta} + 2x_{,\xi}x_{,\eta}y_{,\xi} & y_{,\xi}^2x_{,\eta} + 2x_{,\xi}y_{,\eta}y_{,\xi} \\ x_{,\eta}^2x_{,\xi} & y_{,\eta}^2y_{,\xi} & x_{,\eta}^2y_{,\xi} + 2x_{,\xi}x_{,\eta}y_{,\eta} & y_{,\eta}^2x_{,\xi} + 2x_{,\eta}y_{,\eta}y_{,\xi} \end{bmatrix}. \tag{A.5}$$

Appendix B. The bending stiffness matrix

The effective shear forces may be written as

$$\{Q_n\}^{\mathrm{T}} = \{n\}^{\mathrm{T}} \begin{Bmatrix} \dfrac{\partial M_x}{\partial x} + \dfrac{\partial M_{xy}}{\partial y} \\ \dfrac{\partial M_y}{\partial y} + \dfrac{\partial M_{xy}}{\partial x} \end{Bmatrix} + [x_s \quad y_s] \begin{Bmatrix} \dfrac{\partial M_{sn}}{\partial x} \\ \dfrac{\partial M_{sn}}{\partial y} \end{Bmatrix}. \tag{B.1}$$

Table 7
Non-dimensional natural frequencies of rhombic plates with mixed boundary conditions

θ	Method	N_ξ	Mode sequence				
			1	2	3	4	5
S–S–S–F							
60°	Present	11	14.3162	30.62795	53.0762	59.5763	84.5435
		15	14.2735	30.6520	52.9561	59.5760	84.5960
		17	14.2608	30.6570	52.9261	59.5758	84.6070
	Ref. [27]		14.370	30.969	53.635	61.025	89.704
S–S–S–F							
45°	Present	11	18.6135	36.99612	63.11699	80.7589	98.6931
		15	18.5177	37.0309	63.0552	80.6050	98.5855
		17	18.4975	36.9952	63.0781	80.5590	98.5341
	Ref. [27]		19.054	38.531	66.335	85.897	113.49
S–S–S–C							
45°	Present	11	42.16093	75.0931	111.2095	120.307	153.9386
		15	42.0920	75.0255	111.2435	120.088	153.9490
		17	42.0712	75.0092	111.2435	120.0308	153.9461
	Ref. [28]		41.957	74.948	111.29	119.75	153.94
	Ref. [27]		43.832	76.098	122.40	126.01	193.91
C–C–C–S							
45°	Present	11	57.4720	95.0854	135.2405	144.9885	181.4817
		15	57.4769	95.0224	135.2592	144.9371	181.9943
		17	57.4785	95.0135	135.2782	144.9380	181.9815
	Ref. [28]		57.498	94.991	135.35	145.04	181.96
	Ref. [27]		58.592	96.057	142.98	149.79	217.27
C–C–S–F							
60°	Present	11	18.8225	40.7490	62.2942	73.9588	100.6634
		15	18.7535	40.7327	62.1825	73.9263	100.6890
		17	18.7260	40.7280	62.1610	73.9193	100.6960
	Ref. [27]		18.905	40.973	62.782	75.127	104.41
C–C–C–F							
60°	Present	15	28.9495	47.8431	76.9665	83.7964	109.5119
		17	28.9322	47.8504	76.9084	83.7822	109.5115
		19	28.9200	47.8550	76.8665	83.7695	109.5101
	Ref. [27]		29.025	48.139	77.489	84.895	113.70
C–C–C–F							
45°	Present	15	37.7385	63.3160	93.6345	112.81074	139.5061
		17	37.6380	63.2867	93.5075	112.6985	139.3988
		19	37.5675	63.2698	93.4185	112.6185	139.3240
	Ref. [27]		38.445	64.100	98.385	117.70	151.39

Table 8
Convergence of natural frequencies of trapezoidal plate ($\beta = 0$, $a/b = 1.5$, $b/c = 2.5$)

Boundary type	Method	N_ξ	Mode sequence				
			1	2	3	4	5
S–S–S–S	Present	5	5.4974	15.87790	18.82880	25.91507	27.1004
		7	5.3883	9.338113	14.43305	15.87547	23.3428
		9	5.3891	9.421702	14.70423	15.90912	21.7804
		11	5.3891	9.422411	14.68280	15.90833	21.6956
		13	5.3891	9.422383	14.68202	15.90826	21.6903
		15	5.3891	9.422363	14.68197	15.90827	21.6910
		19	5.3891	9.422346	14.68192	15.90827	21.6909
	Ref. [14]	13	5.3886	9.4228	14.627	15.908	21.683
		15	5.3887	9.4202	14.678	15.909	21.684
		19	5.3889	9.4214	14.678	15.908	21.686
	Ref. [33]		5.3906	9.4311	14.727	15.936	21.909
C–C–C–C	Present	5	10.49059	12.8271	23.6986	25.4883	26.4902
		7	10.47960	15.2972	22.4344	24.6734	34.4001
		9	10.41204	15.5005	21.7013	23.8410	30.7345
		11	10.42700	15.5599	21.4495	23.8919	28.3961
		13	10.42728	15.5636	21.4815	23.9047	28.8791
		15	10.42732	15.5633	21.4756	23.9052	28.8369
		17	10.42732	15.5634	21.4762	23.9053	28.8418
		19	10.42732	15.5634	21.4761	23.9054	28.8415
	Ref. [14]	17	10.427	15.563	21.476	23.905	28.842

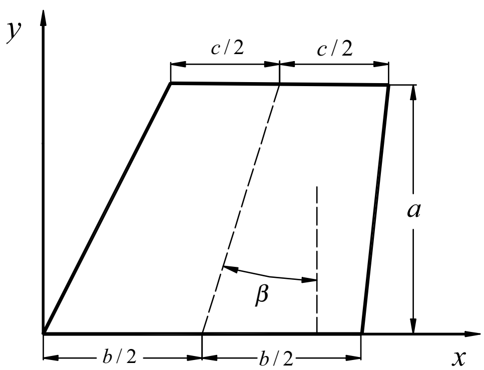

Fig. 3. Geometry of trapezoidal plate.

In the above equation,

$$\{n\}^{\mathrm{T}} = [n_x \quad n_y], \qquad \begin{bmatrix} \dfrac{\partial x}{\partial s} & \dfrac{\partial y}{\partial s} \end{bmatrix} = [-n_y \quad n_x],$$

where n_x, n_y are the components of the unit normal to the boundary of the physical domain. Also, one may note that [23]

$$M_{sn} = n_x n_y(-M_x + M_y) + (n_x^2 - n_y^2)M_{xy} = \{\tilde{n}\}^{\mathrm{T}}\{M\}. \tag{B.2}$$

Table 9
Natural frequencies of simply supported trapezoidal plate for different aspect ratios ($\beta = 0$; $a/b = 1$)

Aspect ratio	Method	N_ξ	Mode sequence							
			1	2	3	4	5	6	7	8
$a/b = 2/3$	Present	11	6.3912	11.938	17.891	18.693	26.578	27.685	34.616	37.262
		13	6.3912	11.938	17.890	18.686	26.732	27.693	34.593	36.431
		15	6.3912	11.938	17.890	18.686	26.738	27.693	34.589	36.339
		17	6.3912	11.938	17.890	18.686	26.738	27.693	34.589	36.337
		19	6.3912	11.938	17.890	18.686	26.738	27.693	34.589	36.337
	Ref. [34]		6.3912	11.938	17.890	18.687	26.742	27.693	34.590	36.346
	Ref. [36]		6.3921	11.940	17.895	18.691	26.746	27.704	34.614	36.350
$a/b = 1/2$	Present	11	1.9400	4.0515	5.0852	7.0013	8.0012	9.9551	10.699	11.971
		13	1.9389	4.0514	5.0823	7.0028	7.9961	9.9570	10.659	12.036
		15	1.9382	4.0514	5.0808	7.0025	7.9959	9.9556	10.658	12.041
		17	1.9377	4.0514	5.0797	7.0023	7.9956	9.9544	10.658	12.041
		19	1.9374	4.0513	5.0790	7.0022	7.9954	9.9536	10.657	12.041
		21	1.9372	4.0513	5.0784	7.0021	7.9953	9.9530	10.657	12.040
	Ref. [34]		1.9569	4.0527	5.1258	7.0095	8.0066	10.007	10.664	12.060
	Ref. [36]		1.9372	4.0540	5.0861	7.0131	8.0086	9.976	10.678	12.103

Table 10
Natural frequencies of simply supported unsymmetric trapezoidal plate ($a/b = 1.5$; $c/b = 0.4$)

β	Method	N_ξ	Mode sequence							
			1	2	3	4	5	6	7	8
10°	Present	11	5.4824	9.4806	14.559	16.350	21.351	23.620	29.480	31.134
		13	5.4824	9.4805	14.557	16.350	21.346	23.615	29.607	31.299
		15	5.4824	9.4804	14.557	16.350	21.346	23.615	29.611	31.307
		17	5.4824	9.4804	14.557	16.350	21.346	23.615	29.611	31.307
		19	5.4824	9.4804	14.557	16.350	21.346	23.615	29.611	31.307
	Ref. [34]		5.4826	9.4825	14.563	16.350	21.354	23.615	29.619	31.309
	Ref. [36]		5.4832	9.4827	14.566	16.356	21.362	23.632	29.66	31.34
20°	Present	11	5.7860	9.6942	14.408	17.513	20.830	24.648	28.521	31.7334
		13	5.7860	9.6938	14.406	17.513	20.820	24.625	28.626	31.8438
		15	5.7859	9.6936	14.406	17.512	20.820	24.624	28.629	31.8474
		17	5.7859	9.6935	14.405	17.512	20.819	24.624	28.628	31.8476
		19	5.7859	9.6934	14.505	17.512	20.819	24.624	28.628	31.8475
		21	5.7859	9.6933	14.505	17.512	20.819	24.624	28.628	31.8475
	Ref. [34]		5.7865	9.6992	14.422	17.516	20.844	24.631	28.652	31.855
	Ref. [37]		5.7881	9.6994	14.424	17.533	20.853	24.688	28.72	32.44

Here,

$$\{\tilde{n}\}^{\mathrm{T}} = [-n_x n_y \quad n_x n_y \quad (n_x^2 - n_y^2)], \quad \{M\}^{\mathrm{T}} = [M_x \quad M_y \quad M_{xy}].$$

Using the constitutive law for bending moments, Eq. (B.2) may be written as

$$M_{sn} = \{\tilde{D}\}^{\mathrm{T}}\{K\}, \tag{B.3}$$

Table 11
Convergence of natural frequencies of fully clamped trapezoidal plate ($\beta = 0$; $a/b = 1$)

Cord ratio	Method	N_ξ	Mode sequence				
			1	2	3	4	5
$c/b = 0.2$	Present	9	11.321	19.696	23.213	30.777	36.854
		11	11.341	19.896	23.311	30.310	36.116
		13	11.341	19.888	23.315	30.348	36.240
		15	11.341	19.888	23.314	30.338	36.224
		17	11.341	19.888	23.314	30.339	36.225
		19	11.341	19.888	23.314	30.339	36.225
		21	11.341	19.888	23.314	30.339	36.225
	Upper bound [39]		11.31	19.77	—	—	—
	Lower bound [39]		11.35	19.93	—	—	—
	Ref. [35]		11.34	19.89	23.31	30.34	36.22
$c/b = 0.4$	Present	9	9.2194	15.508	19.799	24.007	29.116
		11	9.2243	15.584	19.890	24.538	29.174
		13	9.2242	15.582	19.888	24.509	29.195
		15	9.2242	15.582	19.888	24.511	29.193
		17	9.2242	15.582	19.888	24.511	29.193
		21	9.2242	15.582	19.888	24.511	29.193
	Upper bounds [39]		9.23	15.63	—	—	—
	Lower bounds [39]		9.18	15.45	—	—	—
	Ref. [35]		9.224	15.58	19.89	24.51	29.19
$c/b = 0.6$	Present	9	7.5587	13.299	16.641	21.892	23.159
		11	7.5602	13.345	16.709	22.448	23.254
		13	7.5603	13.345	16.708	22.418	23.259
		15	7.5603	13.345	16.708	22.420	23.259
		17	7.5603	13.345	16.708	22.420	23.259
	Upper bounds [39]		7.549	13.27	—	—	—
	Lower bounds [39]		7.571	13.39	—	—	—
	Ref. [35]		7.560	13.35	16.71	22.42	23.26

where

$$\{\tilde{D}\}^{\mathrm{T}} = \{\tilde{n}\}^{\mathrm{T}}[D][\bar{I}], \quad [D] = \begin{bmatrix} D_{11} & D_{12} & D_{13} \\ D_{12} & D_{22} & D_{23} \\ D_{13} & D_{23} & D_{33} \end{bmatrix}.$$

Also, $\{K\}$ and $[\bar{I}]$ are given by Eqs. (30) and (24). The derivative of M_{ns} can be evaluated as

$$\frac{\partial M_{sn}}{\partial x} = \frac{\partial \{\tilde{D}\}^{\mathrm{T}}}{\partial x}\{K\} + \{\tilde{D}\}^{\mathrm{T}}\frac{\partial \{K\}}{\partial x}, \tag{B.4}$$

$$\frac{\partial M_{sn}}{\partial y} = \frac{\partial \{\tilde{D}\}^{\mathrm{T}}}{\partial y}\{K\} + \{\tilde{D}\}^{\mathrm{T}}\frac{\partial \{K\}}{\partial y}. \tag{B.5}$$

Table 12
Convergence of natural frequencies of trapezoidal plates with mixed BCs ($\beta = 0$; $a/b = 1$; $c/b = 0.2$)

Boundary condition	Method	N_ξ	Mode sequence				
			1	2	3	4	5
S–C–S–C	Present	13	7.2944	14.796	17.289	24.743	28.728
		15	7.2945	14.799	17.289	24.748	28.724
		17	7.2945	14.799	17.289	24.748	28.724
		19	7.2945	14.799	17.289	24.749	28.725
		21	7.2945	14.799	17.289	24.749	28.725
	Ref. [34]		7.295	14.80	17.29	24.76	28.72
S–C–S–F	Present	13	7.2301	14.340	17.289	23.088	28.728
		15	7.2307	14.339	17.289	23.091	28.724
		17	7.2311	14.338	17.289	23.091	28.724
		19	7.2314	14.338	17.289	23.092	28.724
		21	7.2316	14.337	17.289	23.092	28.724
	Ref. [31]		7.23	14.36	17.24	23.14	—

For a quadrilateral straight sided plate, the first derivative in the right-hand side of Eqs. (B.4) and (B.5) are zero. Also, in order to do transformation more easily and systematic for programming, one may note that [21]

$$\frac{\partial K}{\partial x} = \begin{bmatrix} 1 & 0 & 0 & 0 \\ 0 & 0 & 0 & 1 \\ 0 & 0 & 1 & 0 \end{bmatrix} \begin{Bmatrix} \dfrac{\partial^3 w}{\partial x^3} \\ \dfrac{\partial^3 w}{\partial y^3} \\ \dfrac{\partial^3 w}{\partial x^2 \partial y} \\ \dfrac{\partial^3 w}{\partial x \partial y^2} \end{Bmatrix}, \quad \frac{\partial K}{\partial y} = \begin{bmatrix} 0 & 0 & 1 & 0 \\ 0 & 1 & 0 & 0 \\ 0 & 0 & 0 & 1 \end{bmatrix} \begin{Bmatrix} \dfrac{\partial^3 w}{\partial x^3} \\ \dfrac{\partial^3 w}{\partial y^3} \\ \dfrac{\partial^3 w}{\partial x^2 \partial y} \\ \dfrac{\partial^3 w}{\partial x \partial y^2} \end{Bmatrix}. \tag{B.6}$$

Using the constitutive law for bending and rearranging its terms, the first term in Eq. (B.1), i.e. Q_n, becomes

$$Q_n = \{\tilde{\tilde{D}}\}^{\mathrm{T}} \begin{Bmatrix} \dfrac{\partial^3 w}{\partial x^3} \\ \dfrac{\partial^3 w}{\partial y^3} \\ \dfrac{\partial^3 w}{\partial x^2 \partial y} \\ \dfrac{\partial^3 w}{\partial x \partial y^2} \end{Bmatrix}, \tag{B.7}$$

where

$$\{\tilde{\tilde{D}}\} = \left\{ \begin{array}{c} (n_x D_{11} + n_y D_{16}) \\ (n_x D_{23} + n_y D_{22}) \\ (3n_x D_{13} + n_y (D_{12} + 2D_{33})) \\ (n_x (D_{12} + 2D_{33}) + 3n_y D_{23}) \end{array} \right\}.$$

Using Eqs. (B.4), (B.5) and (B.6), Eq. (B.1) becomes

$$\{F\}^{\mathrm{T}} \left\{ \begin{array}{c} \dfrac{\partial^3 w}{\partial x^3} \\ \dfrac{\partial^3 w}{\partial y^3} \\ \dfrac{\partial^3 w}{\partial x^2 \partial y} \\ \dfrac{\partial^3 w}{\partial x \partial y^2} \end{array} \right\} = 0, \tag{B.8}$$

where

$$\{F\}^{\mathrm{T}} = \{\tilde{\tilde{D}}\}^{\mathrm{T}} + \frac{\partial x}{\partial s} \{\tilde{D}\} \begin{bmatrix} 1 & 0 & 0 & 0 \\ 0 & 0 & 0 & 1 \\ 0 & 0 & 1 & 0 \end{bmatrix} + \frac{\partial y}{\partial s} \{\tilde{D}\} \begin{bmatrix} 0 & 0 & 1 & 0 \\ 0 & 1 & 0 & 0 \\ 0 & 0 & 0 & 1 \end{bmatrix}.$$

References

[1] C.W. Bert, M. Malik, Differential quadrature method in computational mechanics: a review, Applied Mechanics Review 49 (1996) 1–27.
[2] C.W. Bert, S.K. Jand, A.G. Striz, Two new approximate methods for analyzing free vibration of structural components, American Institute of Aeronautics and Astronautics Journal 26 (1988) 612–618.
[3] S.K. Jang, C.W. Bert, A.G. Striz, Application of differential quadrature to static analysis of structural components, International Journal for Numerical Methods in Engineering 28 (1989) 561–577.
[4] M. Malik, C.W. Bert, Implementation multiple boundary conditions in the DQ solution of higher-order PDEs: application to free vibration of plates, International Journal for Numerical Methods in Engineering 39 (1996) 1237–1258.
[5] X. Wang, C.W. Bert, A new approach in applying differential quadrature and free vibrational analysis of beams and plates, Journal of Sound and Vibration 162 (1993) 566–572.
[6] W. Chen, A.G. Striz, C.W. Bert, A new approach to the differential quadrature method for fourth-order equations, International Journal for Numerical Methods in Engineering 40 (1997) 1941–1956.
[7] X. Wang, H. Gu, Static analysis of frame structures by the differential quadrature element method, International Journal for Numerical Methods in Engineering 40 (1997) 759–772.
[8] T.Y. Wu, G.R. Liu, A differential quadrature as a numerical method to solve differential equations, Computational Mechanics 24 (1999) 197–205.
[9] T.Y. Wu, G.R. Liu, Axisymmetric bending solution of shells of revolution by the generalized differential quadrature rule, International Journal of Pressure Vessel and Piping 77 (2000) 149–157.

[10] T.Y. Wu, G.R. Liu, The generalized differential quadrature rule for fourth-order differential equations, International Journal for Numerical Methods in Engineering 50 (2001) 1907–1929.
[11] G. Karami, P. Malekzadeh, A new differential quadrature methodology for beam analysis and the associated DQEM, Computer Methods in Applied Mechanics and Engineering 191 (2002) 3509–3526.
[12] G. Karami, P. Malekzadeh, Application of a new differential quadrature methodology for free vibration analysis of plates, International Journal for Numerical Methods in Engineering, in press.
[13] X. Wang, A.G. Striz, C.W. Bert, Buckling and vibration analysis of skew plates by the differential quadrature method, American Institute of Aeronautics and Astronautics Journal 32 (1994) 886–889.
[14] C.W. Bert, M. Malik, The differential quadrature method for irregular domains and application to plate vibration, International Journal of Mechanical Sciences 38 (1996) 589–606.
[15] K.M. Liew, J.-B. Han, A four-node differential quadrature method for straight-sided quadrilateral Reissner/Mindlin plates, Communication in Numerical Methods in Engineering 13 (1997) 73–81.
[16] J.-B. Han, K.M. Liew, An eight-node curvilinear differential quadrature formula for Reissner/Mindlin plates, Computer Methods in Applied Mechanics and Engineering 141 (1997) 265–280.
[17] K.M. Liew, J.-B. Han, Bending analysis of simply supported shear deformable skew plates, Journal of Engineering Mechanics 123 (1997) 214–221.
[18] K.M. Liew, J.-B. Han, Bending solution for thick plates with quadrangular boundary, Journal of Engineering Mechanics 124 (1998) 9–17.
[19] F. Civan, Solving multivariable mathematical models by the quadrature and cubature methods, Numerical Methods in Partial Differential Equations 10 (1994) 545–567.
[20] K.M. Liew, F.-L. Liu, Differential cubature method: a solution technique for Kirchhoff plates of arbitrary shape, Computer Methods in Applied Mechanics and Engineering 145 (1997) 1–10.
[21] F.-L. Liu, K.M. Liew, Differential cubature method for static solutions of arbitrary shaped thick plates, International Journal of Solids and Structures 35 (1998) 3655–3674.
[22] C. Shu, B.E. Richards, Application of generalized differential quadrature to solve two-dimensional incompressible Navier–Stokes equations, International Journal of Numerical Methods in Fluids 15 (1992) 791–798.
[23] S.P. Timoshenko, S. Woinowosky Krieger, Theory of Plates and Shells, McGraw-Hill, London, 1970.
[24] A.W. Leissa, The free vibration of rectangular plates, Journal of Sound and Vibration 31 (1973) 257–293.
[25] G. Karami, P. Malekzadeh, Static and stability analysis of arbitrary straight-sided quadrilateral thin plates by DQM, International Journal of Solids and Structures 39 (2002) 4927–4947.
[26] N.S. Bardell, The free vibration of skew plates using the hierarchical finite element method, Journal of Computers and Structures 45 (1992) 841–847.
[27] B. Singh, S. Chakraverty, Flexural vibration of skew plates using boundary characteristic orthogonal polynomials in two variables, Journal of Sound and Vibration 173 (1994) 157–178.
[28] O.G. Macgee, J.W. Kim, Y.S. Kim, A.W. Leissa, Corner stress singularity effects on the vibration of rhombic plates with combinations of clamped and simply supported edges, Journal of Sound and Vibration 193 (1996) 555–580.
[29] K.M. Leiw, Y. Xiang, S. Kitipornchai, C.M. Wang, Vibration of thick skew plates by a variational approach, Journal of Sound and Vibration 168 (1993) 39–69.
[30] T. Mizussawa, T. Kajita, Vibration of skew plates by B-spline functions, Journal of Sound and Vibration 62 (1979) 301–308.
[31] K.M. Liew, K.Y. Lam, A Rayleigh–Ritz approach to transverse vibration of isotropic and anisotropic trapezoidal plates using orthogonal plates functions, International Journal of Solids and structures 27 (1991) 189–203.
[32] X. Wang, Y.L. Wang, R.B. Chen, Static and free vibration analysis of rectangular plates by the differential quadrature element method, Communication in Numerical Methods in Engineering 14 (1998) 1133–1141.
[33] G. Wang, G. Hsu, Static and dynamic analysis of arbitrary quadrilateral flexural plates by B3-spline functions, International Journal of Solids and Structures 31 (1994) 657–667.
[34] K.M. Liew, C.W. Lim, M.K. Lim, Transverse vibration of trapezoidal plates of variable thickness: unsymmetric trapezoids, Journal of Sound and Vibration 177 (1994) 479–501.

[35] K.M. Liew, M.K. Lim, Transverse vibration of trapezoidal plates of variable thickness: symmetric trapezoids, Journal of Sound and Vibration 165 (1993) 45–67.
[36] I. Chopra, S. Durvasula, Vibration of simply-supported trapezoidal plates, Part I. Symmetric trapezoids, Journal of Sound and Vibration 19 (1971) 379–392.
[37] I. Chopra, S. Durvasula, Vibration of simply-supported trapezoidal plates, Part II. Unsymmetric trapezoids, Journal of Sound and Vibration 20 (1972) 125–134.
[38] K.M. Leiw, K.Y. Lam, Application of two dimensional orthogonal plate function to flexural vibration of skew plates, Journal of Sound and Vibration 139 (1990) 241–252.
[39] J.R. Kuttler, V.G. Sigillito, Upper and lower bounds for frequencies of trapezoidal and triangular plates, Journal of Sound and Vibration 78 (1981) 585–590.